CHAPTER- III

MATERIALS, EXPERIMENTAL PROGRAM, METHODS, AND TEST PROCEDURES

3.1 INTRODUCTION

Stabilizing clay is still a difficult task for a variety of construction applications. Based on moisture content and geotechnical properties, clayey and silty clay soils are often categorized as problematic soils with poor geotechnical characteristics. Therefore, for a variety of construction applications, many methods have been employed to enhance the behaviour of problematic soil. One method that is frequently used to stabilize soil within a short span during construction work is chemical stabilization with additives. The demand for energy rises with industrial development, leading to the construction of huge coal-burning power plants. This development creates an issue with the annual safe disposal or beneficial use of massive amounts of fly ash and other byproducts (Zha et al. 2008). However, environmental regulations in several states have recently encouraged the reuse of fly ash and numerous other industrial wastes in an effort to promote sustainable construction. Among these uses are filler or embankment materials; stabilizing agents for soil or aggregates (ACAA 1999). Using fly ash as a soil stabilizing material seems to be one of the many practical solutions to the fly ash waste issue. A more efficient use of fly ash would have a significant positive environmental impact by lowering pollution of the land, air, and water because fly ash is disposed of considerably more frequently than used (Nalbantoglu 2004). There are plenty of examples from the concrete industry demonstrating the effectiveness of nanomaterials. In the past, only a few numbers of applications that stabilized soft soils

using nano additives, lime/cement, and sewage sludge ash were presented in order to highlight their geotechnical characteristics. Additionally, there are some researches available on the potential use of nano silica in pavement wearing courses to investigate the impact on rutting, fatigue, and abrasion resistance. The nano silica treated soil can be used as a chemically stabilized soil for flexible pavement design. For flexible pavement design, it was found that soil stabilized with 6% cement and aqueous colloidal nano silica grade NS-40 satisfied the requirements for chemically stabilized soil (Kulkarni and Mandal 2022). This particular study focused on the utilization of nano silica (NS) along with the industrial waste (fly ash: FA) as an embankment fill material or pavement subgrade. Before application of fly ash and nano silica into the field, a comprehensive analysis under both static and dynamic loading conditions must be carried out because constructing a pavement involves a substantial financial commitment. This chapter discussed the entire experimental testing program that have been conducted in order to meet the objectives of the current investigation. The experimental testing was conducted initially with the chemical characterization, followed by geotechnical, dynamic and small-strain strength characterization. Fig. 3.1 presents the details of the experimental program of the soil combinations. Table 3.1. represents the testing program for physical, chemical, morphological, and geotechnical characteristics of the considered treated and untreated soil combinations. This chapter includes the sources of materials, detailed testing programs, equipment used, and testing procedure.

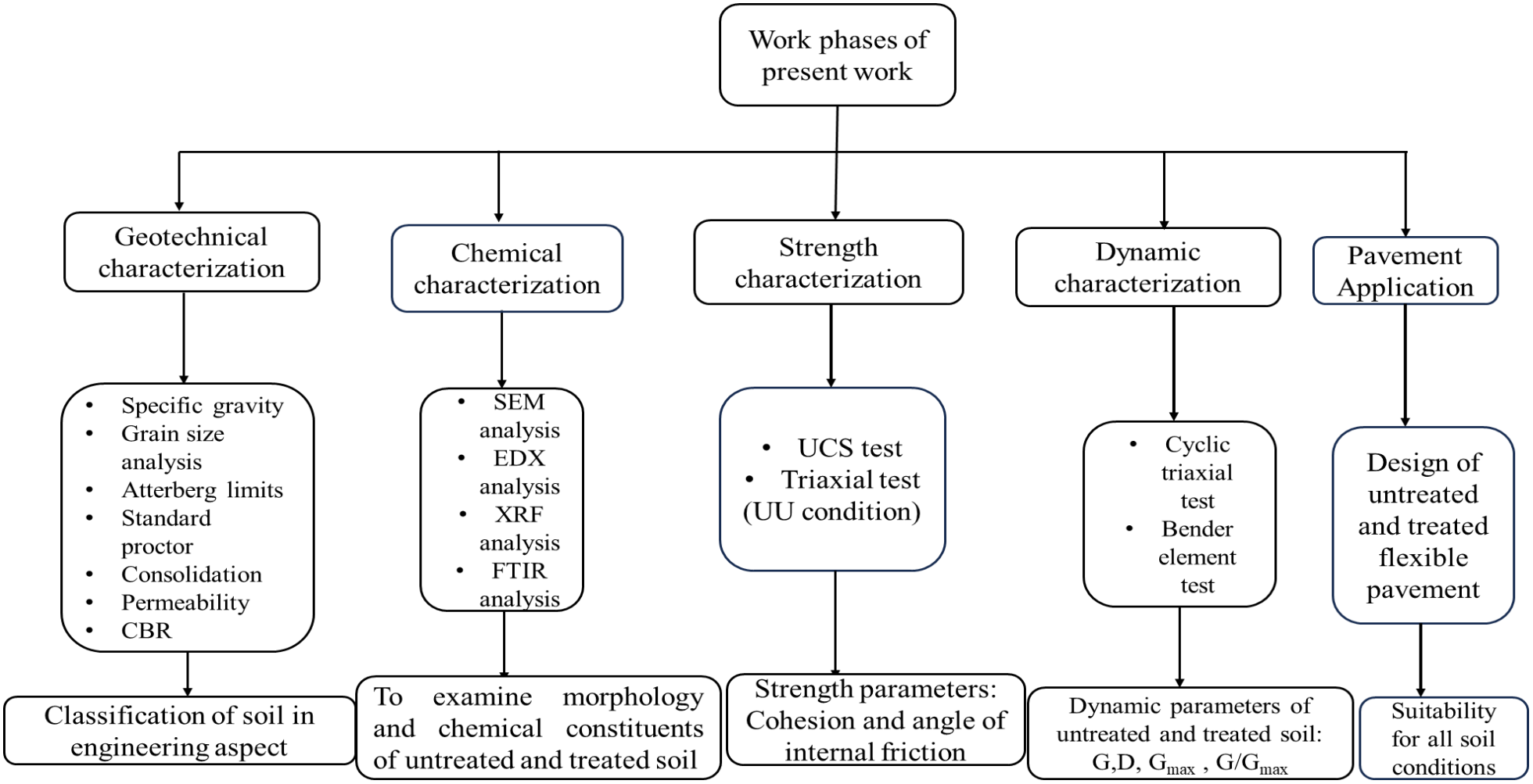

Fig. 3.1 Flowchart of the experimental details of present soil combinations.

3.2 SOURCE OF MATERIALS USED

3.2.1 Source Soil

The soil samples utilized in the investigation were taken from Begusarai, Bihar, at the coordinates of 25° 25' 0.0336" N and 86° 7' 45.7644" E, which is coming in the category of seismic zone-IV (as per IS 1893: Part 1: 2016). Fig. 3.2 depicts the site location of the source soil sample. Bihar is located near the border with Nepal in a high seismic zone on the tectonic plate's edge. Begusarai serves as the administrative centre of the Begusarai district, one of the 38 districts that make up the Indian state of Bihar, as well as the industrial and financial hub of the state. The district is located in India's Mithila area on the northern bank of the Ganges River. Begusarai is located in the centre of the mid-Ganga plain and features low-lying, sloping topography that slopes from south to southeast. Bihar has a wide distribution of loam soils, which are frequently found in the plains with alluvial soils. They can be found in areas of Patna as well as Samastipur and Begusarai district.

3.2.2 Fly Ash

The fly ash in this research was taken from Rihand NTPC (National Thermal Power Corporation) Limited, Uttar Pradesh, India. Fig. 3.2 depicts the site location of the fly ash. The Rihand Super Thermal Power Project is situated in the Indian state of Uttar Pradesh near Renukoot, in the Sonbhadra district. This power station is a coal-based power plant. NTPC Ltd. is the largest power producing company in the nation, and it has built infrastructure at the Rihand facility in Uttar Pradesh to more affordably transport fly ash in bulk quantities to cement facilities that are farther away. The amount of the unburned carbon and other chemical components determine the colour

of fly ash. When the carbon content is high, fly ash is dark grey or black; when the iron content is high, fly ash is tan in colour (Metzger 1987; ACAA, 2003).

3.2.3 Nano Silica

The Nano-SiO_2 (NS) utilized in this research was purchased from Fibrezone, India, Ahmedabad, Gujarat, with a particle size of 12nm, purity of 99.01%, and specific surface area of $200 \pm 25 m^2/g$. It is usually colourless or white and insoluble in ethanol or water. The silica nanoparticles are amorphous and spherical form. Their surfaces can be easily modified to serve a multiple of functions, and they can be made in an extensive range of sizes and forms. Fig. 3.2 depicts the site location of the Nano-SiO_2. The atoms of silicon and oxygen are covalently bound together in silica. Four oxygen atoms have been attached to each silicon atom, and each oxygen atom has shared space with two silicon atoms, respectively. The second most common nanomaterial manufactured worldwide is Nano-SiO_2. As a result, several research studies in the last few decades have concentrated on the possible toxicity and industrial uses of Nano-SiO_2.

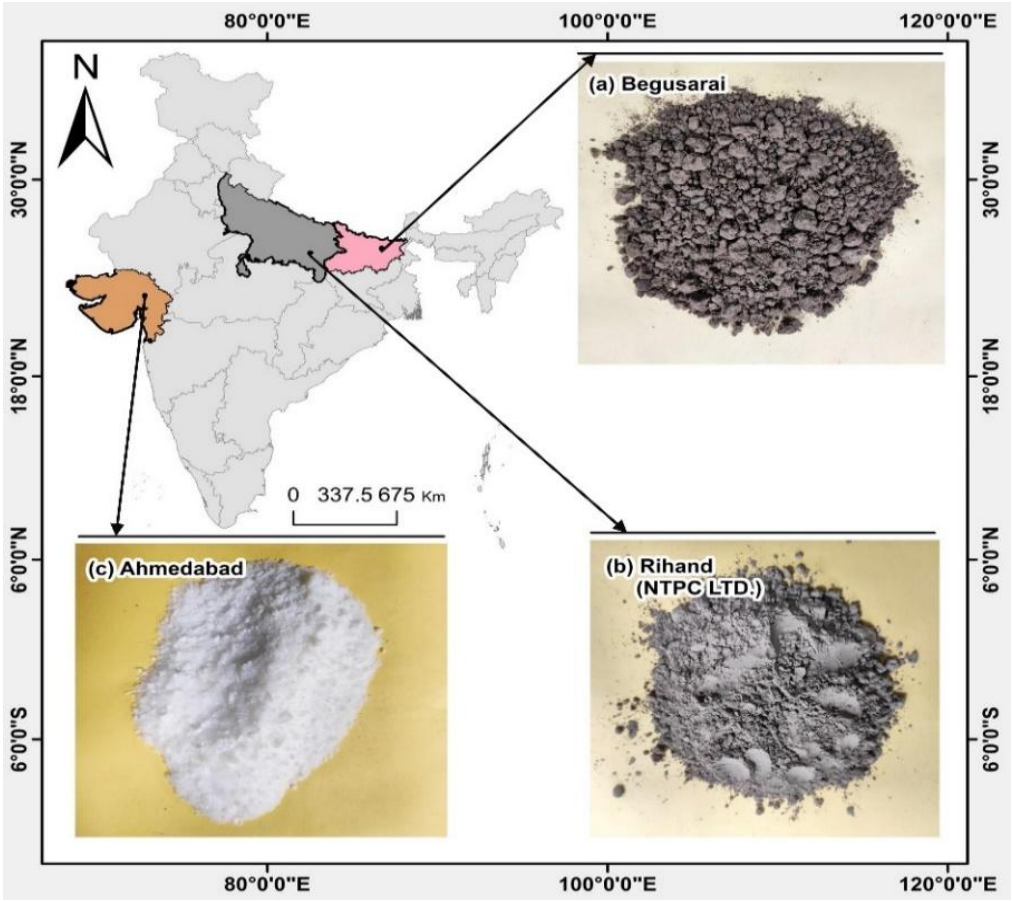

Fig. 3.2. Site locations of the considered materials (a) clay soil (b) fly ash and (c) Nano-SiO_2.

3.3 EXPERIMENTAL PROGRAM

3.3.1Chemical Characterization

3.3.1.1 Scanning Electron Microscope (SEM) Test

The surface morphology of the materials under consideration was examined using a scanning electron microscope (SEM) test. The device that was acquired from CARL ZEISS, Merlin compact with the resolution of 0.8nm @ 15 kV/1.6nm @ 30 kV and magnification range of 12 – 2,000,000x. The scanning electron microscope (SEM) produces a range of signals at the surface of solid specimens by using a focused beam of high-energy electrons. The exterior morphology (texture), chemical composition,

crystalline structure, and the orientation of the components that make up the sample are all revealed by the signals that result from the electron-sample interactions. Most applications involve gathering data over a predetermined portion of the sample's surface and creating a 2-dimensional image to show the spatial differences in these characteristics. SEM uses a dense electron beam to scan the sample's surface, then transforms the signal it receives into greyscale data so that it can be seen on the screen. The resolution of an electron microscope is significantly higher than that of an optical microscope because the electron beam's wavelength is substantially shorter than that of visible light. The optical microscope can only magnify up to 1500 times at its maximum, while the scanning microscope can magnify up to 10,000 times. The instrument's vacuum system keeps the electron optical system operating normally and guards against sample contamination (Xiao et al. 2022).

3.3.1.2 Energy Dispersive X-Ray (EDX) Test

The Energy dispersive X-ray spectroscopy is a method used in the electron microscopy for elemental analysis and the identification of chemical composition of sample. It depends on examining the relationship between a sample and an X-ray excitation source. The EDX test was performed using the facility available at Central Instrument Facility, IIT (BHU) Varanasi. The fundamental idea that every element has a distinct atomic structure, permitting a distinct set of peaks on its X-ray spectrum, is largely responsible for its characterization capabilities. An electron beam is used in a scanning electron microscope (SEM) fitted with an X-ray detector to excite the atoms in a sample. When this beam interacts with the atom, one electron is moved out of its shell and a void is created, which is then filled by an electron with a higher energy level. The energy released in this occurrence is related to certain elements, whilst the proportional counts are related to the element's quantity. Secondary emissions are a

useful tool for differentiating between elements even if some elements may have emission energy overlaps. Since the cumulative spectrum of an element's emission energies is specific to that element, it can be used to identify other particles in a sample that are unknown or to ascertain the composition of the sample.

3.3.1.3 X-Ray Diffraction (XRD) Test

The XRD test was performed using the facility available at Central Instrument Facility (CIF), IIT(BHU), Varanasi. The equipment used was purchased from RIGAKU Corporation (Rigaku Smart Lab 9kW Powder type (without χcradle)). The XRD test works on the principle of Bragg's law. The wavelength of electromagnetic radiation is related to the lattice spacing and diffraction angle in a crystalline sample, i.e., $n\lambda = 2d\sin\theta$, where d = inter atomic distance; θ = angle of diffraction of X-ray; λ = wavelength of the incident X-ray and n = an integer equals to one for first order reflections. As the randomly oriented specimen is scanned over an angular range, the diffractometer detects the intensity of the diffracted beam at precise angles. Because each mineral has a different d-spacing, converting diffraction peaks to d-spacing allows the identification of specific minerals present in the sample. The chemical compounds present in the soil sample were detected with a radiation source of Cu-Kα of wavelength (λ) = 1.540 Å at 40 kV and 35 mA. The entire analysis was conducted in 2θ ranging from 5º to 80º with a step size of 0.02º and the scanning speed was set at 1º per min. The XRD pattern achieved from the test was further analysed using JCPDS-International Centre for Diffraction Data cards.

3.3.1.4 X-Ray Fluorescence (XRF) Spectroscopy Test

The X-ray fluorescence (XRF) spectroscopy is a non-destructive physical technique that can be used to analyse the chemical elements of the materials that are either solid or liquid. This test involves focusing the primary X-ray source on the sample and

using a detector to pick up the fluorescent X-rays that the sample emits. Each element may be recognized by the unique fluorescent X-ray that it emits. Basically, certain electrons are excited by X-ray illumination and move to the next orbital level, then another electron fulfils the gap by producing a fluorescent X-ray. The measurement of this energy helps to identify and determine the percentage of a certain element. This test was performed at the CSIR-Institute of Minerals and Materials Technology (IMMT), Bhubaneswar, India using a Zetium XRF spectrometer with a maximum capacity of 4 kW (Malvern Panalytical, The Netherlands).

3.3.1.5 Fourier Transform Infrared (FTIR) Spectroscopy Test

The FTIR spectroscopy test identifies and describes the chemical compounds of a sample based on their molecular structure by the interaction of a substance with the infrared light. This non-destructive method helps to determine the general composition and functional groups of a sample. The FTIR test was performed using the facility available at Central Instrument Facility (CIF), IIT(BHU), Varanasi. The basic principle of FTIR is that infrared (IR) light from a source is absorbed by a sample. The sample was subjected to a powerful wavelength of infrared light. The FTIR instrument measures the wavelengths of absorption. The Fourier transformation method, which is system-based or generated, aids in the creation of spectral information and is utilized to decode the signal. The sample was placed in the FTIR spectrometer during the testing procedure. A beam of infrared light was directed at the sample to assess its absorbance against IR light at particular frequencies; thin samples work best for examination. The measurement method known as FTIR spectroscopy makes it possible to record infrared spectra. The structure can be established with the great aid of infrared (IR) spectra.

3.3.2 Geotechnical Characterization

3.3.2.1 Specific Gravity

The specific gravity of the soil sample can be measured using a density bottle with a 100 ml capacity fitted with a stopper having a capillary hole. This test has been conducted as per IS:2720 (Part 3) (1989). To conduct this test, about 20 gm of oven-dried soil sample was taken in the density bottle. Initially, the weight of empty density bottle with stopper (W_1) was determined. Then, the weight of bottle filled with soil (W_2) was measured. After adding sufficient air-free distilled water to the density bottle, it was vacuum pumped for 15 minutes to release any entrapped air. After that, the weight of a density bottle that was filled with water and soil (W_3) was measured. Then, the bottle should be cleaned properly after the soil and water have been removed. Then refilled the distilled water in the bottle and weight (W_4) was recorded. The procedure must be carried out at least 3 times in order to calculate the average reading. The specific gravity of the specimen was calculated with the following formula (Eq. 3.1).

$$G_s = \frac{W_2 - W_1}{(W_4 - W_1)(W_3 - W_2)} \tag{3.1}$$

3.3.2.2 Grain Size Distribution

The grain size distribution test was conducted as per IS:2720 (Part 4) (1985). The experiment was conducted using a series of sieves with varying mesh sizes. The arrangement of the sieves is 4.75 mm, 2 mm, 1 mm, 425 µ, 300 µ, 150 µ, 90 µ, and 75 µ respectively. In the current investigation, a wet sieve analysis was carried out by taking required amount of soil sample and thoroughly washing it with distilled water through a 75-micron sieve until the water that passed through the sieve was considerably clear. After washing, the residual coarse parts that were left over 75-

micron were dried in an oven at 105-110°C for 24 hours. Then, the particle size analysis was carried out for the residual coarse portions using mechanical sieve shaker. The aforementioned IS (Indian Standard) sieve setups, which had a pan at the bottom and soil at the top, were arranged on a sieve shaker. Then the soil was sieved for 10 minutes, and the material that remained on each sieve was collected and weighed. Then the grain size distribution curve of the soil was plotted between the percentage finer and the particle size. In the meantime, the passed sample through a 75-micron sieve was collected (50 grams) and treated with deflocculating agents to create a 1000 ml solution with the aid of water. This allowed to ascertain the contribution of silt and clay size particles (0.075 mm to < 0.002 mm). This solution was used to carry out the Hydrometer analysis, which allowed for the theoretical evaluation of the particle diameter and percentage fines.

3.3.2.3 Atterberg Limits

A series of the standard tests known as the Atterberg Limits are used to assess the consistency and plasticity of the fine-grained soils, like silt and clay. These limits, which include the Liquid Limit (LL), Plastic Limit (PL), and Shrinkage Limit (SL), aid in the classification of soils for engineering and construction purposes by evaluating their behaviour when exposed to moisture variations. This test has been conducted as per IS:2720 (Part 5) (1985) and IS: 2720 (Part 6) (1972). In the present study, the liquid limit of the soil and the composite mixtures was measured using the Casagrande liquid limit apparatus. The liquid limit is the minimum water content at which 25 blows to the Casagrande device will cause a soil pat split by a standard-diameter groove to flow together across a distance of 12 mm. The process of determining the plastic limit involves by rolling a clay sample to a 3 mm diameter soil thread. The clay sample breaks during continuous rolling at this size and begins to

lose moisture. The water content at which cracks start to appear is known as the plastic limit. The shrinkage limit was also only found for plastic soil, which was determined by filling the soil sample in the shrinkage dish to a consistency greater than the liquid limit and letting it dry in the air and oven. The shrinkage limit of the soil and composite mixture was ascertained by measuring the change in volume of the shrink soil.

3.3.2.4 Standard Proctor Test

The standard Proctor test determines the maximum unit weight at which a particular type of soil can be compacted at the optimum water content with a controlled compactive force. This test has been conducted as per the IS:2720 (Part 7) (1980). The compaction test was conducted by taking about 2.5 kg of the over-dried soil sample that was thoroughly mixed with the required amount of water. Then this moist soil was poured into the proctor mould in three equal layers, and each layer was compacted with 25 blows using a 2.6 kg rammer that was dropped from a height of 310 mm above the soil. The blows should be distributed equally across the surfaces of each layer. After that, the weight of the compacted soil was measured in order to estimate the bulk unit weight. A representative sample was also retained in order to determine the moisture content. The assessment of the dry unit weight of the sample was aided by the moisture content at a certain trial water content. This procedure was repeated for each increment in moisture content, unless the soil's compacted weight began to decline. After that, in order to determine the maximum dry unit weight and the optimum moisture content of the samples, the plot between dry unit weight and moisture content was plotted.

3.3.2.5 Falling Head Permeability Test

The falling head permeability test can be used to determine the permeability of fine-grained soils, such as silty or clay-like soils. In this experiment, water flows through a soil sample that is attached to a standpipe that measures the water head and volume of water that passes through the sample. This test has been conducted as per the IS:2720 (Part 17) (1986). The oven dried soil sample of 2.5 kg was prepared with the optimum moisture content of soil in order to obtain the required density. After that, using a 2.6 kg dynamic tool, the wet soil was compacted in three layers, giving each layer 25 blows. Then the specimen was saturated by using de-aired water. After attaching the mould's inlet nozzle to the standpipe, the water was let to run until a constant flow was achieved. During the test, the amount of time the water took to drop from the upper to the lower level in the standpipe was recorded. The following formula (Eq. 3.2) was used to determine the coefficient of permeability of the soil sample.

$$K_T = 2.303 \frac{aL}{A(t_f - t_i)} log_{10} \frac{h_1}{h_2} \quad (3.2)$$

where, K_T is the coefficient of permeability, L is the length of the specimen, A is the area of the specimen, a is area of the stand pipe, h_1 and h_2 is the head in the standpipe, and t_f and t_i are the final and initial time respectively.

3.3.2.6 Consolidation Test

The oedometer tests were performed on the soil and the composite mixture to determine the consolidation properties of the samples. The composite samples were prepared using a constant maximum dry density and optimum moisture content of the virgin soil. The consolidation test was conducted as per the IS-2720 (part-15) (1986). A consolidation ring with a height of 20 mm and an internal diameter of 60 mm was used for the test. The rings were coated inside with silicon grease to lessen side

friction between the ring and the side specimen. To ensure there was no air entrapment in the specimens, they were manually remoulded in the consolidation rings. Subsequently, the consolidation ring was covered with a porous stone. To stop particles from being forced into the porous stones, filter sheets were placed in between the specimens. The ring was then inserted into the loading frame, placed inside a consolidation cell, and immersed in distilled water at a 5 kPa seating pressure. At loading increments of 25, 50, 100, 200, 400, and 800 kPa, the stresses were applied. After every loading phase, the settlement was monitored for 24 hours. After the maximum loading was applied, the stresses were released in the reverse order.

3.3.2.7 Unconfined Compressive Strength (UCS) Test

The soil samples were first oven-dried and then prepared for UCS test as per the IS: 2720 (Part-10) (1991). A cylindrical mould with dimensions of 38 mm in diameter and 76 mm in height was used for the UCS test. An unconfined compression test is one in which the soil specimen is not kept laterally confined. A dial gauge and proving ring-equipped load frame were used to measure the axial deformation and axial load, respectively. The tests were carried out at a strain rate of 1.2 mm/min and continued loading until failure or an early 20% axial strain, whichever came first. In order to prevent moisture from evaporating, the specimens were cured for 1, 7, 14, and 28 days at room temperature within the sealed plastic bags. The stress-strain plot yields the maximum axial stress that leads to failure, which is the unconfined compressive strength of the soil. The unconfined compressive strength of the specimen is the average of the three specimens obtained by repeating the procedure for a minimum of three specimens. Table 3.1 Illustrates the details of the UCS test.

3.3.2.8 Triaxial Shear Test

The static triaxial (Unconsolidated Undrained) test was conducted to measure the undrained shear strength parameters of the soil and composite mixture. For the triaxial (UU) test specimen, a cylindrical split mould with a diameter of 38 mm and two detachable collars was used to ensure specimen homogeneity in the 76 mm height of cylindrical mould. The strain-controlled procedure outlined in IS 2720 (part 11) (1993) was followed in regulating the triaxial tests. Initially, the specimen was placed in a triaxial cell and a confining pressure was applied using water. After that, the specimen was exposed to shearing under undrained compression loading conditions by applying a constant rate of deformation. The tests were conducted at different confining pressures (50 kPa, 100 kPa, and 150 kPa) at an axial loading rate of 1.2 mm/min. The loading was continued until the specimen failed or an early 20% axial strain occurred, whichever came first. Table 3.1 Illustrates the details of the triaxial test.

3.3.2.9 California Bearing Ratio (CBR) Test

The soil samples were first oven-dried and then prepared for CBR test as per the IS: 2720 (Part-16) (1987). The California Bearing Ratio (CBR) is the ratio of the force per unit area needed to penetrate a soil mass at a rate of 1.25 mm/min using a circular plunger with a 50 mm diameter compared to the same amount of force needed to penetrate a standard material. The ratio is typically calculated for 2.5 mm and 5 mm penetration. The ratio at 5 mm is utilized when it consistently exceeds the ratio at 2.5 mm. The load readings at penetrations of 0.5, 1.0, 1.5, 2.0, 2.5, 4.0, 5.0, 7.5, 10 and 12.5 mm was recorded. After that, a load penetration curve was plotted. The corrected load value is found by applying the load-penetration curve to the desired penetration value, and the CBR is then calculated as follows (Eq. 3.3).

California Bearing Ratio= $\frac{P_T}{P_S} \times 100$ (3.3)

where, P_T = Corrected unit (or total) test load corresponding to the chosen penetration from the load penetration curve, and P_S= unit (or total) standard load for the same depth of penetration.

3.3.3 Dynamic Characterization

3.3.3.1 Cyclic Triaxial Test

3.3.3.1.1 Description of the Equipment

In the present study a computerized semi-automated cyclic triaxial testing (CXT) equipment with both static and cyclic loading facility supplied by M/s. HEICO, New Delhi, India was used. The apparatus comprises a submersible load cell with a capacity of ±5 kN and an accuracy of 0.001 kN, as well as a displacement transducer with limits of ±50 mm and ±10 mm, both with an accuracy of 0.01 mm. The reverse side of the triaxial cell base is equipped with pore pressure transducers, which have an accuracy of 1.0 kPa and a range of 0–2,000 kPa. The triaxial cells with sample sizes ranging from 38 mm to 100 mm in diameter and a length to diameter ratio of 2:1 can be accommodated by the load frame. In order to apply the necessary flow and pressure to the hydraulic actuator, a hydraulic power supply is included in the system. Using the compressed air generated by the air compressor, the pneumatic control panel guarantees precise confining and back pressure application. With an external input, the device can be configured to operate in a frequency range of 0.01 Hz to 10 Hz, producing a variety of waveforms, including sine, triangle, rectangular, and square. Fig. 3.3 shows the details of the cyclic triaxial testing (CXT) equipment used in the present study.

Fig. 3.3. (a) Cyclic triaxial test apparatus, (b) Data acquisition system, and (c) Prepared sample.

3.3.3.2 Sample Preparation for Cyclic Triaxial Test

The CTX test was conducted using the remoulded cylindrical specimens of 50 mm in diameter and 100 mm in height. The samples were prepared using the moist tamping technique in accordance with the compaction characteristics of the soil. Many researchers have used the moist tamping procedure for silty and clay type of soil (DeGregorio 1990; Pandya and Sachan 2018). First, the required amounts of the additives were dry mixed to prepare mix for the samples. The necessary amount of moisture was then gradually added using a sprayer, and the mixture was stirred until it was completely homogeneous. Subsequently, three equal layers of moist mixtures were poured into the cylindrical mould, and each layer was individually compacted to obtain the required MDD. After levelling both ends of the prepared sample, a plunger was used to extrude it. In order to preserve the moisture during the curing process, it was weighed and then sealed in the airtight plastic bag.

3.3.3.3 Testing Procedure of Cyclic Triaxial Test

The CTX tests (under consolidated undrained condition) were conducted as per the ASTM D3999 and ASTM D5311 standards. Initially, the circular filter paper of the same size was laid over the saturated porous stone disc, which had the same diameter as of the sample, and the disc was set on top of the triaxial testing machine pedestal. The specimen was positioned over the filter paper. After being stretched in the membrane stretcher, the rubber membrane was placed on the soil sample. To stop cell water from getting inside the soil specimen, O-rings were provided at the top and bottom of the platens. After that, the triaxial cell was positioned over the base and screwed firmly. After the sample is prepared and mounted, the triaxial test typically consists of three steps: saturation, consolidation, and shearing. After the sample was placed in the triaxial cell, the saturation process was carried out by gradually raising the back pressure while maintaining the effective confining pressure at 20 kPa. The Skempton's pore water parameter B ($B = \frac{\Delta u}{\Delta \sigma_c}$ where Δu = change in pore pressure and $\Delta\sigma_c$ = change in confining pressure) as also routinely checked until a value of 0.95 was obtained, signifying that the specimen was nearly saturated. After reaching more than 95% saturation, the material was isotopically consolidated to the required effective confining pressure. The consolidation is considered to be finished if the volume change reading shows no variation and the pore pressure stays constant throughout that time. A hydraulic actuator was used to apply strain-controlled cyclic loading to the sample in a vertical direction following the consolidation procedure. In the strain-controlled CTX experiment, the soil and composite mixture soil samples were sheared. At different shear strain (γ) of 0.6%, 0.9%, 1.2%, 1.5%, 2.1%, 2.4%, 2.7%, and 3.0%, multiple sets of CTX (CU) tests were carried out with 28 days curing period. Finally, the axial deformation, cyclic load, confining pressure, pore water

pressure, and number of cycles were all recorded using the data acquisition system. The findings of the previous studies were taken into consideration when choosing the loading frequency and shear strain amplitudes for the current work (Thomas and Rangaswamy 2020). Table 3.2 Illustrates the details of testing program considered for the cyclic triaxial test. A total of 48 CTX tests were performed with an effective confining pressure of (σ'_c) 100 kPa, a loading frequency of (f) 1 Hz, and varying cyclic shear strain. Although there are several loading frequencies at which the cyclic triaxial testing can be performed, multiple researchers selected and used the 1 Hz loading frequency (Thomas and Rangaswamy 2020; Vardanega and Bolton 2013; Subramaniam and Banerjee 2020, Naik et al. 2022).

The dynamic properties of geo-materials, namely their dynamic shear modulus (G) and material damping ratio (D), are crucial parameters of the ground response analysis in geotechnical engineering problems. Fig. 3.4 depicts a typical stress-strain response of the hysteresis loop for cyclic loading condition (Sitharam et al. 2004). The G is the slope of a line formed between shear stress and shear strain that goes from the origin to the hysteresis loop's maximum and minimum peaks. Additionally, the D is estimated following the computation of the area of the hysteresis loop, representing the energy dissipation, and the area of the shaded region, representing the stored potential energy. From Eq. 3.4, Young's modulus (E) can be estimated with the help of the hysteresis loop. Eqs. 3.5-3.7 can be used for the evaluation of shear modulus (G), shear strain (γ), and damping ratio (D).

$$E = \frac{\sigma_d}{\varepsilon} \tag{3.4}$$

$$G = \frac{E}{2(1+\nu)} \tag{3.5}$$

$$\gamma = (1+\nu)\varepsilon \text{ and} \tag{3.6}$$

$$D = \frac{A_L}{(4\pi A_T)} \tag{3.7}$$

where, γ=shear strain; ε=axial strain; ν=poisons ratio (for saturated undrained conditions assumed to be equal to 0.5); A_L= area covered by the hysteresis loop; and A_T= area of the triangular portion.

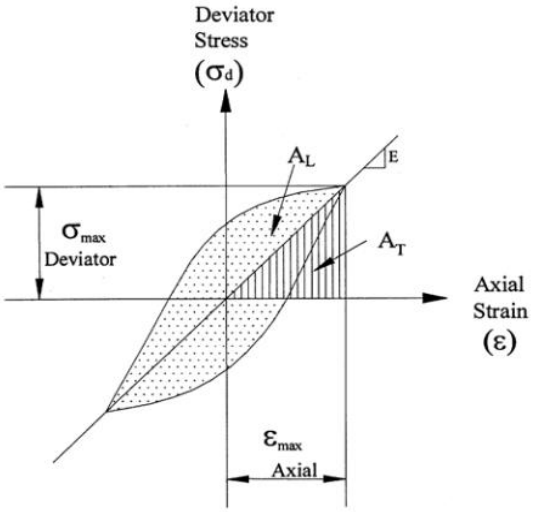

Fig. 3.4. A schematic stress-strain hysteresis loop for cyclic loading (Sitharam et al. 2004)

3.3.4 Small-Strain Shear Modulus Characterization

3.3.4.1 Bender Element (BE) Test

The BE test is the most reliable non-destructive test to evaluate the small-strain shear stiffness ($\gamma < 10^{-5}$) of soil. The usage of piezoelectric bender elements for determining the shear wave velocity was probably introduced by Shirley 1978; Shirley and Hampton 1978. Fig. 3.5 illustrates the details of the Bender Element test apparatus. The bender element test was conducted in accordance with the ASTM D8295-19. The bender element apparatus consists of two thin piezoceramic plates, known as the transmitter and receiver, which are firmly held together by a central conductive metal shim. Due to the piezoceramic properties, the bender element deforms when activated by an input voltage potential and generates a mechanical vibration. Bender elements

are responsible for converting mechanical vibration into output electrical voltage and vice versa (Leong et al. 2009). Bender elements behave to transmit and receive the shear waves through the soil samples. The small-strain shear modulus of the specimens can be evaluated by the following correlation (Eq. 3.8).

$$G_{max} = \rho V_s^2 \tag{3.8}$$

where, ρ= bulk density of soil; and V_s = shear wave velocity.

In order to evaluate the shear wave velocity (V_s) using bender element tests, the travel distance and the travel time through the soil sample need to be measured. The shear wave velocity of the specimens can be evaluated by using the equation (Eq. 3.9) given below.

$$V_s = \frac{L_{tt}}{t} \tag{3.9}$$

where, L_{tt}=travel distance and t=travel time of the shear waves between transmitter and receiver. Table 3.3 Illustrates the details of Bender Element test. Several approaches have been suggested for the analysis of the bender element test results including the time domain (TD) and the frequency domain (FD) techniques (Viana da Fonseca et al. 2009; Camacho-Tauta et al. 2015, Kawaguchi et al. 2016). There are three approaches to ascertain the arrival time in time domain technique. The first method involves measuring the difference between the transmitted and received wave signals to determine the propagation time in the soil specimen, as shown in Fig. 3.6 (a) (Jovičić et al. 1996). The second technique, which is illustrated in Fig. 3.6 (b), involves calculating the cross correlation (C.C.) between the transmitted and received waves (Mancuso et al. 1989; Viggiani and Atkinson 1995). The amplitude and phase angle relations with frequency axis are produced by the third approach, which computes the cross spectrum of the transmitting and receiving waves, as shown in

Fig. 3.6 (c). The arrival time is then calculated using the inclination of the phase spectrum. Because it utilizes the frequency characteristics of the input and output waves, it is commonly referred to as the frequency domain technique (F.D) (Blewett et al. 1999; Greening and Nash 2004).

The time domain techniques include applying input sine-wave pulses at different frequencies, such as the specimen-BE system's particular resonance frequency, and using the first-direct-arrival approach to compute the travel time. The travel time of the shear wave can be computed using the cross-correlation (C.C.), start-to-start (S.S.), and peak-to-peak (P.P.) approaches. The start-to-start (S.S.) method refers to the time interval between the transmitted wave's starting point and the corresponding point in the received wave. The peak-to-peak (P.P.) method refers to the time interval between the transmission wave's peak point and the corresponding peak in the received wave. The C.C. technique is used to compute the shear wave arrival time by using the Eq. 3.10. The arrival time is determined at the location of the highest peak of correlation if the largest amplitude signal is the one that is received first. The required arrival time is calculated by picking the initial peak in the C.C. time history rather than the peak with the maximum amplitude when the reception peak is not the highest one.

$$CC_{xy}(\tau) = \lim_{T=\infty} \frac{1}{T} \int_T X(t).Y(t+\tau)d\tau \qquad (3.10)$$

Where, $CC_{xy}(\tau)$: cross correlation function, T: recording period, $X(t)$: time history of input wave, $Y(t)$: time history of received wave, τ: delay.

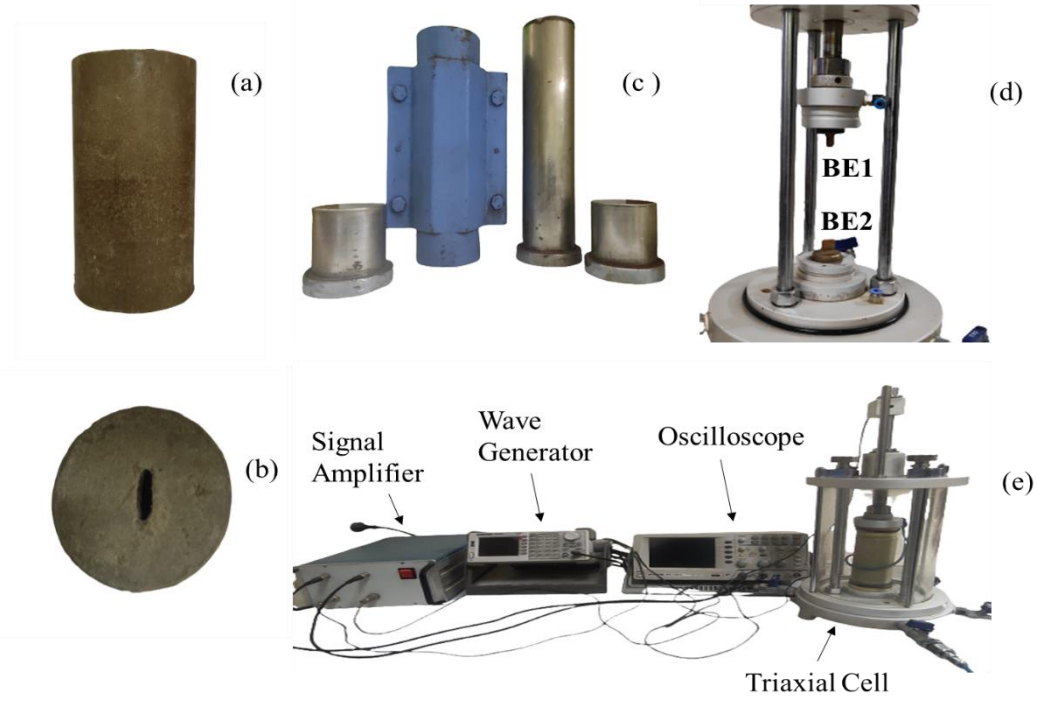

Fig. 3.5. Bender Element test facility: (a) Typical prepared sample (b) Typical grooving sample (c) Cylindrical mould with accessories (d) Bender Element as Transmitter and Receiver (e) Bender Element test set up with triaxial cell.

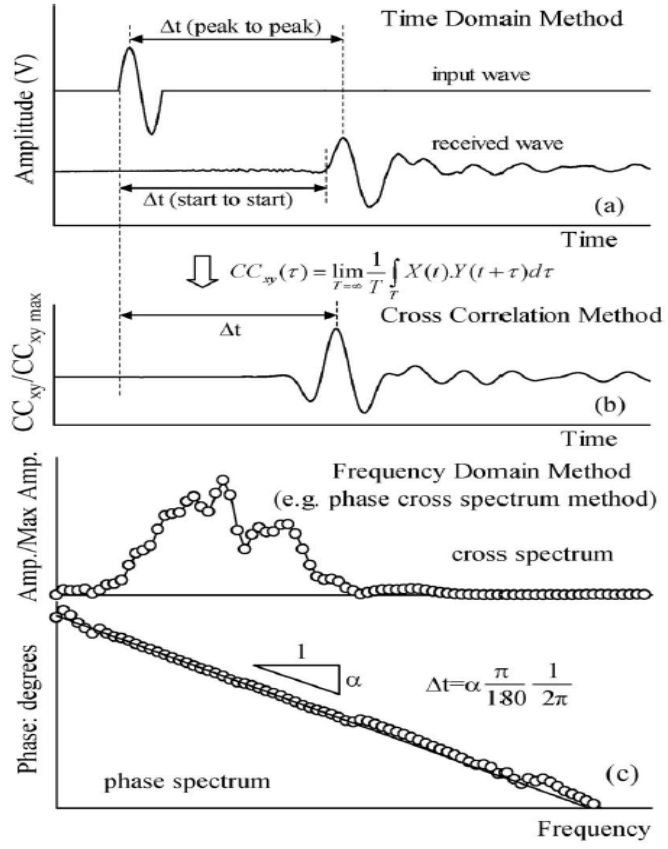

Fig. 3.6. Typical identification methods of travel time; (a) time domain method, (b) cross correlation method and (c) frequency domain method (Yamashita et al. 2009).

The specimens for the bender element testing were prepared using the same cylindrical mould, which has a 50 mm diameter and a 100 mm height, as in the case of cyclic triaxial test. The remoulded test specimens were prepared at the optimal soil water content to get the same maximum dry density in order to examine the efficacy of the binders on the soil matrix. In the current research, the travel time under various confining pressures of 50 kPa, 100 kPa, and 150 kPa was proposed to be the distance between the start to start (in the time domain) of the transmitted and the received wave. Fig. 3.7 illustrates the typical shear wave travel from the BE test.

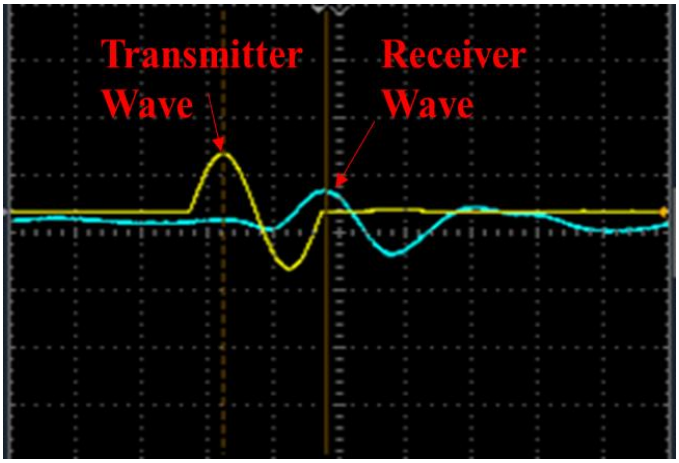

Fig. 3.7. Typical shear wave travel from the BE test.

3.3.5 Testing Program

The purpose of the aforementioned studies, which included morphological, mineralogical, chemical, and geotechnical properties as well as sample preparation, was to classify and identify the samples based on their physical, chemical, and geotechnical characteristics. Initially, static tests were conducted to ensure the continuity of the research. Once the optimum results were found, cyclic triaxial and bender element tests were conducted. The optimal results decide the final application of the stabilizing additives in the field. Therefore, the study focused on the optimal results of the additives. Several static triaxial (Unconsolidated Undrained) tests using

the mixture of Nano-SiO_2 and fly ash were carried out after the optimal Nano-SiO_2 dosages were obtained. The fly ash dosages used were 10%, 20%, and 30% by the weight of the parent soil. The strain-controlled CTX and BE experiments were performed after getting the optimum 1% Nano-SiO_2 and 20% fly ash dosages. Several sets of CTX (Consolidated Undrained) tests were conducted at varying shear strain (γ) of 0.6%, 0.9%, 1.2%, 1.5%, 2.1%, 2.4 %, 2.7%, and 3.0% at a curing age of 28 days.

Thomas and Rangaswamy 2020 assessed the high plasticity clay using a strain-controlled cyclic triaxial test with cyclic strain amplitudes ranging from 0.15 to 3.375. The results showed that stabilization increases the shear modulus and damping ratio of the soil because it increases the amount of stress dissipation, and the energy absorption brought about by particle densification, pore volume reduction, and greater bonding between the cemented particles. Similarly, Thakur et al. 2020 investigated the dynamic behaviour of low plasticity cohesive soil with varied stress histories (Over Consolidation Ratio of 1, 2, 3, and 4) as well as with the varied cyclic axial strain amplitude of 0.5%, 1%, 1.5%, and 2% under strain-controlled cyclic triaxial testing.

Therefore, here the consolidated undrained cyclic triaxial testing with higher cyclic shear strain was conducted using the cyclic triaxial setup. The detailed schematic explanation of the bender element and cyclic triaxial test schedule have been presented below.

Table 3.1. Testing program for physical, chemical, morphological, and geotechnical characteristics.

Material	Experiments	Details of experiments	No. of tests
Clayey soil and fly ash (FA)	Physical	Specific gravity tests	2
	Morphological and Chemical	Scanning electron microscope (SEM) test	2
		Energy Dispersive X-Ray (EDX) test	2
		X-Ray Diffraction (XRD) test	2
		X-Ray Fluorescence (XRF) Spectroscopy test	1
		Fourier Transform Infrared (FTIR) Spectroscopy test	1
	Geotechnical	Grain size distribution	2
		Atterberg limits test	2
		Standard Proctor compaction test	2
		Falling head permeability test of clayey soil	1
		Consolidation tests of clayey soil	1
		Unconfined Compressive Strength (UCS) test of clayey soil	3
		Static triaxial (UU) tests of clayey soil under confining pressures of 50, 100 & 150 kPa	3
		California Bearing Ratio (CBR) test of clayey soil	2
Mix 1: Clayey soil treated with Nano-SiO_2 (NS)	Geotechnical	Atterberg limits test at NS=0.5, 1, 3, 5, and 7%	5
		Compaction tests at NS=0.5, 1, 3, 5, and 7%	5
		Unconfined Compressive Strength (UCS) test at NS=0.5, 1, 3, 5, and 7% at different curing days (0,1,7,14,28)	75
		Static triaxial (UU) tests at NS=0.5, 1, 3, 5, and 7% at different curing days (0,1,7,14,28)	75
		California Bearing Ratio (CBR) test at NS=1% (optimum)	2
		Falling head permeability test at NS=1% (optimum)	1
		Consolidation tests at NS=1% (optimum)	1
	Morphological and Chemical	Scanning electron microscope (SEM) test at NS=1% (optimum)	1
		Energy Dispersive X-Ray (EDX) test at NS=1% (optimum)	1
		X-Ray Diffraction (XRD) test at NS=1% (optimum)	1
		X-Ray Fluorescence (XRF) Spectroscopy test at NS=1% (optimum)	1
		Fourier Transform Infrared (FTIR) Spectroscopy test at NS=1% (optimum)	1

Mix 2: Clayey soil treated with fly ash (FA) + 1% Nano-SiO_2 (NS)	Geotechnical	Atterberg limits test at NS: 1%, FA: 10, 20, 30%	3
		Compaction tests at NS: 1%, FA: 10, 20, 30%	3
		Static triaxial (UU) tests at NS: 1%, FA: 10, 20, 30% at different curing days (0,1,7,14,28)	45
		California Bearing Ratio (CBR) test at NS=1% & FA: 20% (optimum) at different curing days (0,28)	4
		Falling head permeability test at NS=1% & FA: 20% (optimum)	1
		Consolidation tests at NS=1% & FA: 20% (optimum)	1
	Morphological and Chemical	Scanning electron microscope (SEM) test at NS=1% & FA: 20% (optimum)	1
		Energy Dispersive X-Ray (EDX) test at NS=1% & FA: 20% (optimum)	1
		X-Ray Diffraction (XRD) test at NS=1% & FA: 20% (optimum)	1
		X-Ray Fluorescence (XRF) Spectroscopy test at NS=1% & FA: 20% (optimum)	1
		Fourier Transform Infrared (FTIR) Spectroscopy test at NS=1% & FA: 20% (optimum)	1
Total test performed			257

Table 3.2. Testing program for cyclic triaxial (CU) test.

SL No.	Combinations	Curing period (days)	Frequency (Hz)	Effective confining pressure (kPa)	Strain amplitudes (%)	No of tests
1	Clay	0, 28	1	100	0.6, 0.9, 1.2, 1.5, 2.1, 2.4, 2.7, 3.0	16
2	Clay+1% NS	0, 28	1	100	0.6, 0.9, 1.2, 1.5, 2.1, 2.4, 2.7, 3.0	16
3	Clay+1% NS+20% FA	0, 28	1	100	0.6, 0.9, 1.2, 1.5, 2.1, 2.4, 2.7, 3.0	16
Total test performed						48

Table 3.3. Testing program for bender element test.

SL No.	Combinations	Curing period (days)	Frequency (kHz)	Effective confining pressure(kPa)	No of tests
1	Clay	0	1, 2	0, 50, 100, 150	8
2	Clay+1% NS	0,1,7,28	1, 2	0, 50, 100, 150	32
3	Clay+1%NS+10%FA	0,1,7,28	1, 2	0, 50, 100, 150	32
4	Clay+1%NS+20%FA	0,1,7,28	1, 2	0, 50, 100, 150	32
5	Clay+1%NS+30%FA	0,1,7,28	1, 2	0, 50, 100, 150	32
Total test performed					136